

This is the accepted manuscript made available via CHORUS. The article has been published as:

Antiproton stopping in H_2 and H_2O

J. J. Bailey, A. S. Kadyrov, I. B. Abdurakhmanov, D. V. Fursa, and I. Bray

Phys. Rev. A **92**, 052711 — Published 25 November 2015

DOI: [10.1103/PhysRevA.92.052711](https://doi.org/10.1103/PhysRevA.92.052711)

Antiproton stopping in H_2 and H_2O

J. J. Bailey, A. S. Kadyrov, I. B. Abdurakhmanov, D. V. Fursa, and I. Bray

*Curtin Institute for Computation and Department of Physics, Astronomy and Medical Radiation Sciences,
Curtin University, GPO Box U1987, Perth 6845, Australia*

Stopping powers of antiprotons in H_2 and H_2O targets are calculated using a semiclassical time-dependent convergent close-coupling method. In our approach the H_2 target is treated using a two-center molecular multiconfiguration approximation, which fully accounts for the electron-electron correlation. Double ionization and dissociative ionization channels are taken into account using an independent-event model. The vibrational excitation and nuclear scattering contributions are also included. The H_2O target is treated using a neonization method proposed by Montanari and Miraglia [*J. Phys. B* **47** 015201 (2014)], whereby the ten-electron water molecule is described as a dressed Ne-like atom in a pseudo-spherical potential. Despite being the most comprehensive approach to date, the results obtained for H_2 only qualitatively agree with the available experimental measurements.

PACS numbers: 34.10.+x, 34.50.Bw

I. INTRODUCTION

The study of energy loss as heavy charged particles travel through matter is of fundamental importance in many fields including medical radiation therapy [1], aviation and space exploration [2], and astrophysics [3]. The development of sources of low energy antiprotons is drawing significant attention to the area of antiproton scattering from atoms and molecules, see the review of Kirchner and Knudsen [4]. With potential application to radiotherapy and oncology, interest in the processes occurring during antiproton scattering from atoms and molecules is growing (see, e.g., Refs. [5, 6]).

Stopping power measurements for antiprotons in a gas of H_2 were first performed by Adamo *et al.* [7] at the CERN LEAR facility. To obtain the stopping power they first simultaneously measured the spatial coordinates and annihilation times of antiprotons traveling through a gas of H_2 . The measured quantities are then expressed in terms of the stopping power with the resulting equations solved numerically using parameters to obtain the best fit to the data. Agnello *et al.* [8] later repeated the experiment using the same technique due to errors in the pressure scale of the original measurements. This led to significantly different results, thus superseding the earlier ones given by Adamo *et al.* [7]. Lodi Rizzini *et al.* [9] later reanalyzed the data with emphasis on the Barkas effect [10].

From a theoretical perspective, Bethe [11] was the first to develop a quantum-mechanical approach to calculating stopping powers in atomic targets. However, his general formula is applicable only at sufficiently high projectile energies due to the first Born and dipole approximations used in the approach. When Bethe theory is applied to molecules Bragg's additivity rule [12] is usually used. With significant developments in the field of hadron therapy the importance of highly accurate calculations of heavy projectile interactions with matter has been growing. The most recent calculations of antiproton stopping in H_2 have been performed by Lühr and

Saenz [13]. They used a semiclassical close-coupling approach to the solution of the time-dependent Schrödinger equation. The radial wave function was expanded in a B-spline basis with the H_2 target described using an effective one-electron treatment. Poor agreement with the experiment of Agnello *et al.* [8] was obtained. However good agreement with the original (incorrect) data of Adamo *et al.* [7] was seen. Lühr and Saenz [13] concluded that a two-electron description of H_2 was required to reduce uncertainties in the calculations and also test the accuracy of the latest experimental measurements. The only other H_2 calculations available have been performed by Schiwietz *et al.* [14, 15] using a quasi-atomic generalized adiabatic-ionization (AI) method which is valid at low energies.

There are a number of calculations for antiproton stopping in atomic hydrogen. These are usually compared with the experimental data for its molecular counterpart divided by two. Schiwietz *et al.* [14, 15] performed calculations using atomic-orbital close coupling and distorted-wave Born methods, while Cabrera-Trujillo *et al.* [16] used electron nuclear dynamics (END) formalism. Both concluded that disagreement with experiment around and below the stopping maximum was due to neglecting molecular structure effects in their calculations.

Recently we have applied a semiclassical time-dependent convergent close-coupling (CCC) method to calculations of antiproton stopping powers in the atomic targets of H, He, Ne, Ar, Kr, and Xe [17]. For H we obtained excellent agreement with other theoretical calculations while for He our results were in best agreement with experiment when compared to other theories. In this paper we extend the method to antiproton stopping in the molecular targets of H_2 and H_2O . The results presented in this paper improve upon the current theory of Lühr and Saenz [13] by employing a correlated two-electron multiconfiguration molecular treatment of H_2 and taking into account double ionization and dissociative ionization via an independent-event model. In addition, we include vibrational excitation and the so-called nuclear

stopping power. When calculating the dominant electronic stopping power we use an analytic orientation averaging technique to account for all possible orientations of the H_2 molecule and compare this to the average over three orientations.

The H_2O target is treated using a neonization method proposed by Montanari and Miraglia [18], whereby the ten-electron water molecule is described as a dressed Ne-like atom in a pseudo-spherical potential. To our best knowledge there have been no other stopping power calculations for the antiproton- H_2O system. Our calculations should provide a guideline to future experiments on antiproton stopping in H_2O .

The paper is set out as follows. Section II outlines the method. The results of calculations are presented in Section III. Section IV discusses the status of the experiment and theory. Finally in section V we draw conclusions.

II. TIME-DEPENDENT CONVERGENT CLOSE-COUPLED METHOD IN IMPACT-PARAMETER REPRESENTATION

The time-dependent CCC method has been applied to calculations of ionization cross sections for antiprotons incident on H_2 [19, 20] and H_2O [21]. Here we summarize the method for these targets.

A. H_2 target

A semi-classical impact-parameter approach is used whereby the relative motion of the incident antiproton is treated classically however the target electrons are treated fully quantum mechanically. The antiproton is assumed to have a straight line trajectory $[\mathbf{R}(t) = \mathbf{b} + \mathbf{v}t]$ where \mathbf{v} is velocity and \mathbf{b} is impact parameter. We expand the total (electronic) scattering wave function in terms of a complete set of target pseudostates Φ_α , that is

$$\Psi(t, \mathbf{r}, \mathbf{R}, \mathbf{d}) = \sum_{\alpha} A_{\alpha}(t, \mathbf{b}, \mathbf{d}) \exp(-i\epsilon_{\alpha}t) \Phi_{\alpha}(\mathbf{r}, \mathbf{d}), \quad (1)$$

where ϵ_{α} is the energy of the target electronic state α , \mathbf{R} is the position vector of the antiproton relative to the target center of mass, \mathbf{r} collectively denotes the position vectors of all target electrons, and \mathbf{d} is the relative coordinate of the target nuclei in the laboratory frame. The probability for transitions into electronic bound and continuum states are defined by the expansion coefficients A_{α} . Substitution of the total scattering wave function (1) into the time-dependent Schrödinger equation yields a set of coupled-channel differential equations for the expansion coefficients A_{α} , which are solved with the condition that the target is initially in the ground state. In order to find orientation-averaged transition probabilities we factor out the orientation-dependent parts from our

equations and after analytically integrating over all orientations of the molecular axis we obtain a system of differential equations for the orientation-independent part of the scattering amplitudes $\mathcal{A}_{\alpha\lambda\mu}$. Orientation-averaged probabilities for transition of the target from the ground state to some final state f at fixed internuclear distance d are then defined by

$$p_f(b) = \sum_{\lambda\mu} \frac{1}{2\lambda+1} |\mathcal{A}_{f\lambda\mu}(t = +\infty, b, d)|^2, \quad (2)$$

where λ and μ are limited by the maximum allowed total orbital angular momentum and b is the magnitude of the impact parameter. Scattering cross sections are obtained as the integral of the probability over impact parameters:

$$\sigma_f = 2\pi \int_0^{\infty} p_f(b) b db. \quad (3)$$

For H_2 target structure calculations the Born-Oppenheimer approximation is utilized with the internuclear distance fixed at the ground-state equilibrium value of $d = 1.4487$ a.u.. Target pseudostates $\Phi_{\alpha}(\mathbf{r})$ are obtained via diagonalization of the H_2 Hamiltonian in a set of antisymmetrized two-electron configurations constructed from one-electron orbitals. These orbitals are built using Laguerre functions,

$$\xi_{kl}(r) = \left[\frac{\lambda_l(k-1)!}{2(k+l)(k+2l)!} \right]^{1/2} (\lambda_l r)^{l+1} \times \exp(-\lambda_l r/2) L_{k-1}^{2l+1}(\lambda_l r), \quad (4)$$

where $L_{k-1}^{2l+1}(\lambda_l r)$ are the associated Laguerre polynomials, l is the orbital angular momentum and index k ranges from 1 to N_l , the maximum number of Laguerre functions. The exponential fall-off parameter λ_l is typically chosen to be optimal for the ground state. Specific values of λ_l used for each target are given below. With this choice of basis we can model the whole spectrum of the target molecule. As N_l is increased the negative-energy pseudostates converge to the true discrete eigenstates, while the positive-energy pseudostates yield an increasingly dense discretization of the target continuum. In this work we use a multiconfiguration approach, meaning we allow several inner electron orbitals in our two-electron configurations. Specifically, we include the $1s$, $2s$, $2p$, $3s$, $3p$, and $3d$ orbitals for the description of the inner electron. The number of one-electron states of the outer electron are as large as required to ensure converged results. For more details refer to Ref. [20].

B. H_2O target

For the H_2O target we reduce the multi-center problem to a central one using a neonization method proposed by Montanari and Miraglia [18], whereby the water molecule is described as a dressed pseudo-spherical

atom. With molecular orientation dependence removed from the problem the probability for transition of the target from the ground state to some final state f becomes

$$p_f(b) = |A_f(t = +\infty, b)|^2. \quad (5)$$

The aforementioned neonization technique has recently been used in the time-dependent CCC formalism by Abdurakhmanov *et al.* [21]. Embracing the ideas of Ref. [18] we approximate the multi-center nuclei Coulomb potential of H_2O with the spherical potential

$$V_{\text{H}_2\text{O}} = -\frac{8}{r} - \frac{2(1-\eta)\Theta(R_{\text{H}} - r)}{R_{\text{H}}} - \frac{2(1-\eta e^{1-r/R_{\text{H}}})\Theta(r - R_{\text{H}})}{r}, \quad (6)$$

where Θ is the Heaviside step function, R_{H} is the distance between the oxygen atom and either of the two hydrogen atoms, and η is introduced to account for the deviation of the target potential from spherical symmetry and is varied to match the experimentally measured value for the ground state ionization energy of H_2O . Now that a multi-center problem has been reduced to a central one we can apply the techniques used to determine the structure of the Ne atom. Therefore the H_2O molecule is represented by the same model that we have previously used for Ne [17]: six p -shell electrons above a frozen Hartree-Fock core with only one-electron excitations from the outer p shell allowed. Additionally, the core wave functions for the Ne atom are replaced by the appropriate H_2O core wave functions which are taken from the Slater basis representation presented in [18].

C. Stopping power

The stopping power is the energy loss per unit path length and is defined as

$$-\frac{dE}{dx} = NS(E_0), \quad (7)$$

where $S(E_0)$ is referred to as the stopping cross section and is related to the stopping power by the number of target molecules per cubic meter, N . Here E_0 is the incident energy of the projectile. When using the semi-classical approximation for calculations involving heavy projectiles the total stopping cross section is the sum of two contributions, the nuclear and the electronic stopping cross sections.

The electronic contribution is the energy losses associated with all events leading to excitation, ionization and dissociation of the target. As described in our previous work [17], the electronic stopping cross section in the CCC formalism is defined as

$$S_e(E_0) \approx \sum_{f=1}^{N_{\text{T}}} (\epsilon_f - \epsilon_i) \sigma_f + \sum_{k=1}^{N_{\text{T}}^+} (\epsilon_k - \epsilon_i^+) \sigma_k^+, \quad (8)$$

where σ_f is the scattering cross section for transition of the target electron from the ground state of energy ϵ_i to some final state f of energy ϵ_f , and N_{T} (N_{T}^+) is the total number of H_2 (H_2^+) pseudostates included in the calculation. In addition to single non-dissociative ionization and excitation, the present calculations of the stopping cross section for H_2 include energy losses due to double ionization and dissociative ionization of the H_2 target. Dissociative ionization takes place through single ionization followed by dissociation of the residual H_2^+ . These processes are represented by the second term in Eq. (8), where ϵ_i^+ is the ground state energy of H_2^+ , and σ_k^+ is the cross section for the transition of the inner electron to a state k of energy ϵ_k .

For calculations of double ionization (DbI) and dissociative ionization (DiI) we employ an independent-event model, where these processes are considered in a two-step approximation. The first step is single ionization of H_2 and the second is ionization or excitation of H_2^+ . Therefore the cross section is defined by the product of the total single ionization probability of H_2 , $p_{\text{ion}}^{\text{H}_2}$, and the probability of H_2^+ transitioning from the ground state to some final state k , i.e

$$\sigma_k^+ = 2\pi \int_0^\infty p_{\text{ion}}^{\text{H}_2}(b) p_k^{\text{H}_2^+}(b) b db. \quad (9)$$

Antiproton collisions with H_2^+ are modeled in much the same way as for H_2 , as described in Sec. II A. However, in this case H_2^+ pseudostates and the appropriate interaction potential are used. We also use the same internuclear distance as for H_2 calculations, as required by the independent-event model. The cross sections corresponding to the positive-energy states of H_2^+ represent double ionization, while those corresponding to the negative energies contribute towards dissociative ionization due to the repulsive nature of the H_2^+ excited states.

The nuclear stopping cross section S_n is the contribution from momentum transfer to the target during elastic and inelastic scattering. This contribution is included in our antiproton- H_2 calculations to compare with experiment, which measures all energy loss contributions at once. To calculate the nuclear stopping cross section we first construct the angular differential cross section from the impact parameter amplitudes via the Bessel transformation,

$$\frac{d\sigma_f(\mathbf{d})}{d\Omega} = (\mu v)^2 \left| \int_0^\infty A_f(b, \mathbf{d}) J_{m_f}(2\mu v b \sin \frac{1}{2}\theta) b db \right|^2, \quad (10)$$

where μ is the reduced mass of the projectile-target system, v is the lab-frame incident velocity, J is the Bessel function of the first kind, m_f is the magnetic quantum number, and θ is the scattering angle. The resulting differential cross section is orientation dependent. We use averaging over three perpendicular orientations to calculate the differential cross section $d\sigma_f/d\Omega$ independent of the target orientation. As discussed later averaging over

three orientations is sufficiently accurate at energies below 30 keV. The nuclear stopping cross section is then given by

$$S_n(E_0) = \sum_f \int \frac{q_f^2}{2m_t} \left(\frac{d\sigma_f}{d\Omega} \right) d\Omega, \quad (11)$$

where m_t is the mass of the target and q_f is the magnitude of momentum transfer to the target which depends on the scattering angle. Finally, we emphasize that our amplitude A_f entering Eq. (10) contains the information about the heavy-particle interaction. Though this is not essential for the electronic part of the stopping power, it is not possible to get the correct differential cross section without including the projectile interaction with the target nuclei.

Collisions between antiprotons and molecular hydrogen also result in changes in vibrational energy levels of the target. These processes lead to an additional loss of the projectile's energy. Their contribution to the stopping cross section can be accounted for if we write the total scattering wave function in a form where its nuclear and electronic parts are separated as

$$\Psi(t, \mathbf{r}, \mathbf{R}, \mathbf{d}) \chi_{f,\nu}(\mathbf{d}), \quad (12)$$

where $\chi_{f,\nu}(\mathbf{d})$ is the molecular vibrational wave function that depends on the internuclear distance of the target in the electronic state f . As discussed in [20] this kind of separation is possible under the assumption that the electrons can almost immediately adjust their positions to a changed nuclear configuration. The wave functions and corresponding energies for the vibrational motion of the molecular target, $\chi_{f,\nu}(\mathbf{d})$ and $\varepsilon_{f,\nu}$, satisfy the following Schrödinger equation:

$$(H_{\text{nucl}} + \epsilon_f) \chi_{f,\nu}(\mathbf{d}) = \varepsilon_{f,\nu} \chi_{f,\nu}(\mathbf{d}), \quad (13)$$

where H_{nucl} is the target Hamiltonian representing nuclear motion. The stopping cross section associated with the vibrational transitions from the electronic ground state i into all the vibrational levels of the electronic state f can be calculated as

$$S_{\text{vib},f}(E_0) = \frac{1}{4\pi} \sum_{\nu=0}^{N_{\text{vib},f}} (\varepsilon_{f,\nu} - \epsilon_{i,0}) \times |\langle \chi_{f,\nu}(\mathbf{d}) | A_f(t, \mathbf{b}, \mathbf{d}) \exp(-i\epsilon_f t) | \chi_{i,0}(\mathbf{d}) \rangle|^2, \quad (14)$$

where $N_{\text{vib},f}$ is the total number of molecular vibrational eigenstates in the electronic state f . Among all vibrational transitions, those within the electronic ground state give the most dominant contribution to the stopping cross section. Thus, in the present work we consider vibrational transitions only within the electronic ground state. To avoid doing averaging over molecular orientations numerically we write Eq. (14) in the following

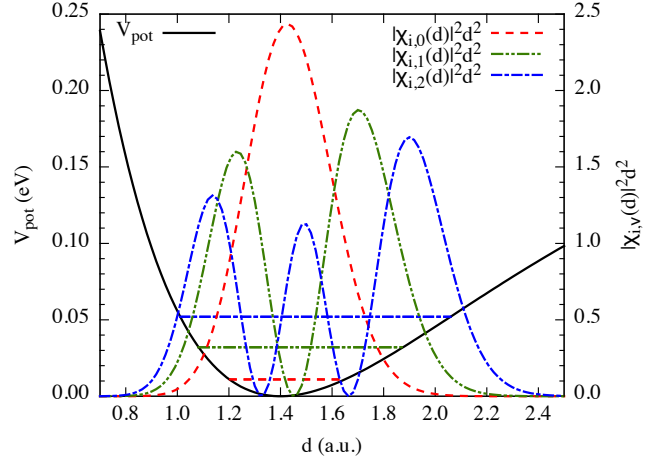


FIG. 1. Radial distribution functions $|\chi_{i,\nu}(d)|^2 d^2$ of the H_2 molecular vibrations with $\nu = 0, 1$, and 2 , in a.u.. The potential energy curve and the vibrational energy levels of H_2 are shown in units of eV. Note that the potential energy curve is shifted up by 31.7007 eV which is the ground state energy of H_2 at the equilibrium internuclear separation of 1.4487 a.u..

approximate form

$$S_{\text{vib}}(E_0) \approx \sum_{\nu=0}^{N_{\text{vib},i}} (\varepsilon_{i,\nu} - \epsilon_{i,0}) \langle \chi_{i,\nu}(d) | \sqrt{\sigma_{\text{el}}^{\text{av}}(d)} | \chi_{i,0}(d) \rangle, \quad (15)$$

where $\sigma_{\text{el}}^{\text{av}}(d)$ is the elastic cross section analytically averaged over molecular orientations. Using $\sqrt{\sigma_{\text{el}}^{\text{av}}(d)}$ instead of the scattering amplitude is shown to be a good approximation in calculations for electron scattering from H_2^+ and D_2^+ [22]. The molecular vibrational eigenfunctions $\chi_{i,\nu}(\mathbf{d})$ and eigenenergies $\varepsilon_{i,\nu}$ can be calculated via diagonalization of the molecular Hamiltonian with the electronic ground-state potential curve V_{pot} . In Fig. 1 radial distribution functions, $|\chi_{i,\nu}(d)|^2 d^2$, for the lowest vibrational levels ($\nu = 0, 1$ and 2) are given.

III. RESULTS

A. \bar{p} in H_2

For calculations of the electronic stopping cross sections for antiprotons in H_2 we find that the maximum orbital angular momentum of the target states l_{max} required to reach convergence is 5, which is the same for H_2^+ . For both H_2 and H_2^+ sufficient convergence is obtained for $N_l = 20 - l$ with λ_l chosen to be 2. A total of 843 molecular target states are included in our antiproton- H_2 calculations. With this model we obtain a two-electron ground state ionization energy of 1.16497 a.u., which is close to the accurate value of 1.1745 a.u. [23]. Calculations were performed for the internuclear

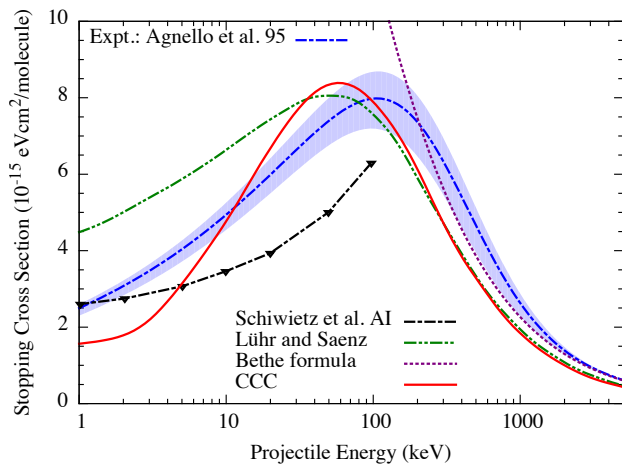


FIG. 2. Total stopping cross section for antiproton incident on molecular hydrogen. Included is the experimental data of Agnello *et al.* [8], with the shaded region representing the experimental uncertainty. The CCC results are shown by the solid line. The electronic stopping cross sections of Lühr and Saenz [13] and Schiwietz *et al.* [14, 15] are also shown, along with the results from Bethe formula. Results previously presented per atom have been multiplied by two.

separation of 1.4487 a.u. The same internuclear separation was used in the H_2^+ calculations as required by the independent-event model.

In Fig. 2 we present results for the antiproton- H_2 stopping cross section together with the theoretical calculations of Lühr and Saenz [13] and Schiwietz *et al.* [14, 15], as well as the experimental results of Agnello *et al.* [8]. We use an analytic orientation-averaging technique to account for all possible orientations of the molecule. We also take into account double ionization and dissociative ionization via the independent-event model. The nuclear and vibrational-excitation contributions are also added, which make a noticeable contribution below about 10 keV, as discussed in more detail later. The CCC results are in good agreement with those of Lühr and Saenz [13] above 200 keV. However below 30 keV our calculations are in better agreement with the experimental measurements. Note that the results of Lühr and Saenz [13] do not include the nuclear contribution. Adding the latter would further worsen their disagreement with the experiment below 10 keV. The calculations of Schiwietz *et al.* [14, 15] also do not include the nuclear contribution. Additionally, both Lühr and Saenz [13] and Schiwietz *et al.* [14, 15] use an atomic approximation to molecular hydrogen.

It is important to point out that traditionally the \bar{p} - H_2 stopping cross section has been presented per atom instead of per molecule. In Fig. 2 we present our final result as per molecule and therefore multiply other per-atom results by two before plotting.

Individual contributions to the total stopping cross section are presented in Fig. 3. First, the figure shows

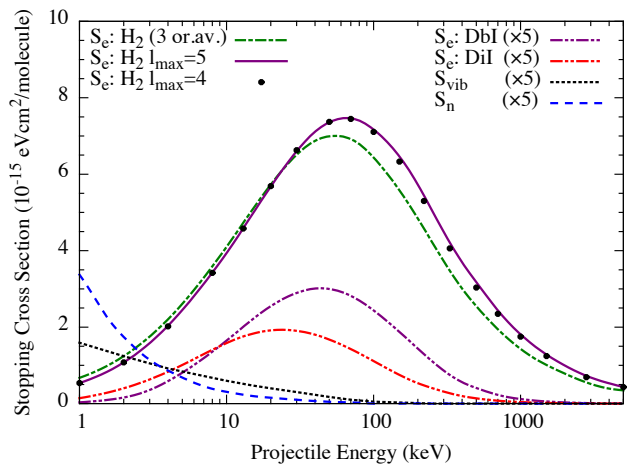


FIG. 3. Individual contributions to the antiproton- H_2 total stopping cross section. The solid curve labeled $S_e: H_2$ is the stopping cross section for the primary electron analytically averaged over all possible molecular orientations with $l_{max} = 5$. The dots are the same but with $l_{max} = 4$. Similarly $S_e: H_2$ (3 or.av.) is for an average over just three perpendicular orientations. $S_e: DBI$ and $S_e: DI$ are the stopping cross sections associated with double ionization and dissociative ionization (obtained using analytic orientation averaging technique). S_n is the nuclear stopping cross section and S_{vib} is the vibrational-excitation contribution.

the level of convergence when the maximum orbital angular momentum of the target states l_{max} reaches 5. Second, the figure shows that energy losses associated with double ionization and dissociative ionization processes make a small but important contribution, as does the nuclear stopping cross section. Energy loss to vibrational excitation is shown to make a small contribution at low energies. All these components are multiplied by a factor of 5 to make them visible in comparison with the dominant electronic contribution. The nuclear and vibrational-excitation stopping cross sections make negligible contribution above 10 keV. For the nuclear stopping cross section we increase the number of the final states of the target until a convergent result is obtained. Interestingly, as the number of states are increased the contribution to the total nuclear stopping cross section for elastic scattering is reduced and distributed into other channels. Nevertheless, the elastic contribution remains dominant.

Fig. 3 also demonstrates the improvement an analytic orientation averaging technique for the target molecule provides over averaging using three orientations. When compared to averaging over three perpendicular orientations, analytic averaging over all possible target orientations significantly increases the stopping cross section near and above the stopping maximum, and slightly reduces it below about 10 keV. The stopping cross section for each of the three orientations used in Fig. 3 are presented in Fig. 4. These three perpendicular orientations

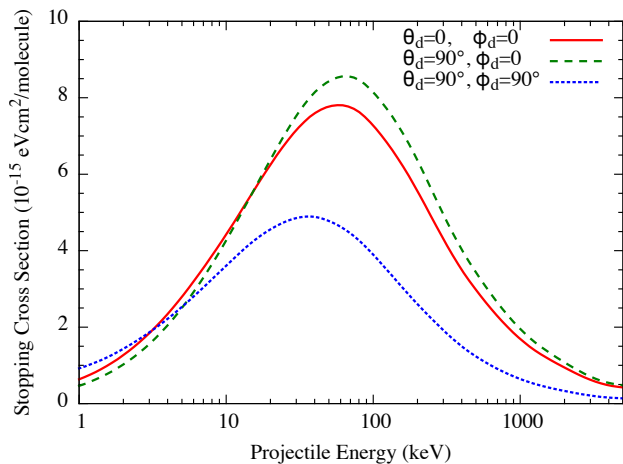


FIG. 4. Electronic stopping cross section for one electron excitations from three main orientations of the H_2 molecule for antiprotons.

of the target molecule are shown in the key of Fig. 4.

In Fig. 5 we compare the electronic part of the antiproton- H_2 stopping cross section obtained in the present CCC method with those obtained in various approximate theoretical treatments of the molecular target. We show results we have obtained using a H-like (single active electron) structure model for H_2 . In this model we choose the atomic number Z_{eff} of the hydrogen atom to reproduce the correct one-electron ground state energy of H_2 . These results are then multiplied by two to account for both electrons of the molecule. These results are in good agreement with our full calculations above 150 keV. In this figure we also show the results of Lühr and Saenz [13]. Their calculations were also performed using a H-like H_2 structure model, however they introduced a model potential instead of simply varying Z_{eff} . After multiplication by two there is good agreement with our calculations above 200 keV. The disagreement at low energies between our full CCC calculations and those using a H-like structure model is attributed to the lack of electron-electron correlation effects in the latter which demonstrates the importance of using a proper molecular structure model. Additionally, in Fig. 5 we show our previous calculations for atomic hydrogen [17] multiplied by 1.8. This factor is determined by fitting to our H_2 results at high energies and demonstrates a slight deviation from Bragg's additivity rule [12] due to bonding effects. With this factor there is agreement with our full molecular calculations above 150 keV.

B. \bar{p} in H_2O

We have also performed electronic stopping cross section calculations for antiprotons in H_2O using a frozen-core neonization treatment proposed in [18] with $N_l =$

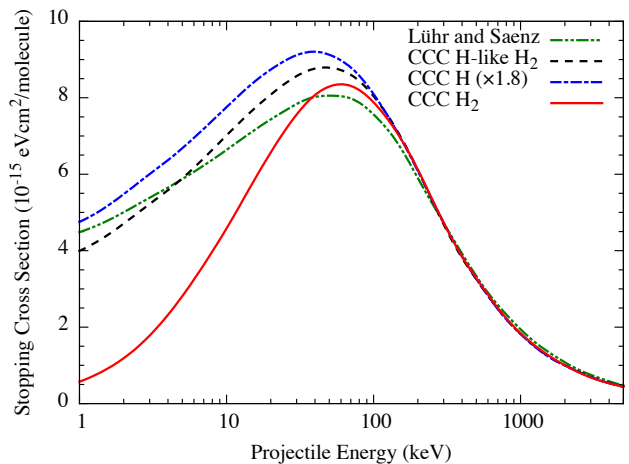


FIG. 5. Comparison of the electronic stopping cross sections obtained using the full molecular approach and various H-like approximations.

$20 - l$ and λ_l chosen to be 2. The maximum orbital angular momentum of target states used in calculations was 4. This resulted in the total number of coupled differential equations being 1112.

The present results for H_2O are shown in Fig. 6. There is no experiment and to our best knowledge there have been no other calculations for the antiproton- H_2O system. However, the demand for calculations of antiprotons stopping in biologically important molecules such as water is rapidly increasing due to current research such as the Antiproton Cell Experiment (ACE) [5, 6] at CERN. The ACE aims to fully assess the suitability and effectiveness of antiprotons for cancer therapy. While our calculations for H_2O using a neonization approximation can not be considered highly accurate, they should still provide a guideline to future experiments on antiproton

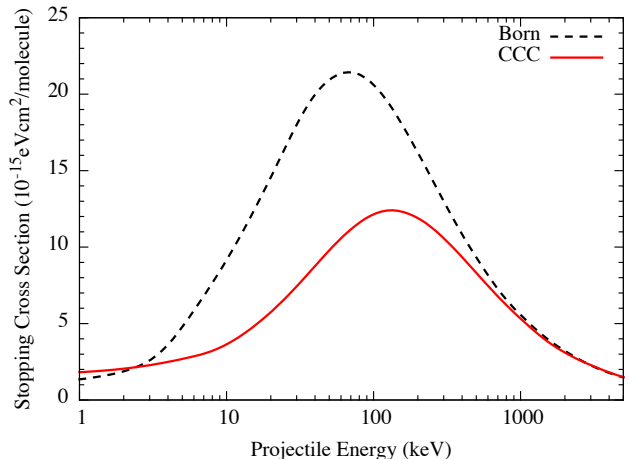


FIG. 6. Electronic stopping cross sections for antiproton in H_2O .

stopping in this target. We note that the presented curve is the stopping cross section associated with the energy losses due to single electron transitions from the outer p -shell only. It represents the dominant contribution to the stopping cross section. The present Born approximation results are also shown.

IV. DISCUSSION

We have developed the most comprehensive approach to calculating the stopping cross section of antiprotons in H_2 to date. Nevertheless, as can be seen from Fig. 2 there is still some disagreement between the experiment and calculations. In order to better understand the reason for the disagreement we analyze the situation from the theoretical point of view. We start by mentioning that our theory uses the independent-event model to include the double-ionization and dissociative-ionization channels. This model tends to overestimate the double-ionization and dissociative ionization cross sections. However since the contribution of these processes to the total stopping cross section is small they should not have a significant effect on the presented final results.

Secondly, we do not include direct homolytic dissociation of the target. To our best knowledge there are no calculations of this process induced by antiprotons that could be used to estimate its contribution to the energy loss. However, according to Khayrallah [24] electron-impact direct dissociation of H_2 takes place through doubly-excited states of the target. This in turn means that the process is a two-electron one and its probability is significantly smaller than the probability of the single-electron processes. If we assume that antiproton-induced direct dissociation of H_2 also goes via doubly-excited states, then one can expect that its contribution to the total stopping cross section will be small, possibly similar to the contribution of the dissociative ionization (see Fig. 3). As far as direct heterolytic dissociation is concerned, the probability of this happening is even smaller.

It is also important to emphasize that the main reason behind the small stopping power cross section obtained in the present calculations at low energies is the strong suppression of the ionization cross section. This target structure-induced suppression of ionization has a well-understood theoretical basis [4, 19].

As a cross test of the present results we note that when the internuclear distance of the computer code for H_2 is set to zero our previous He calculations [17], which are in better agreement with experiment at low energies than for H_2 , are perfectly reproduced. All the above gives us a certain degree of confidence in the reliability of the presented results.

Finally, we would like to make a comment about the experimental method, which we believe may also contribute to the disagreement between the experiment and

calculations. The experiment of Agnello *et al.* [8] measures the mean annihilation time $\langle t_a \rangle$ and path length R for antiprotons traveling through a H_2 gas chamber. Both measured quantities are expressed as integrals over functions of the total stopping cross section S . These two relationships are solved simultaneously by making use of a parameterized function for S presented by Andersen and Ziegler [25] for atomic targets. At high energies the function is based on Bethe's formula and is given by $S_h = [(243 - 0.375Z_t)Z_t/E_0] \ln(1 + \gamma/E_0 + 4m_e E_0/m_{\bar{p}} \bar{E})$, where Z_t is the atomic number of the target taken to be 1, m_e and $m_{\bar{p}}$ is the electron and antiproton mass respectively, and \bar{E} is the mean excitation energy of the target. At low energies it is given by $S_l = \alpha E_0^\beta$ which is based on the Thomas-Fermi statistical model. In the intermediate energy range the interpolation formula $1/S = 1/S_l + 1/S_h$ is used, which was originally proposed by Varelas and Biersack [26]. The variables α , β , and γ are varied to fit the experimentally measured data for $\langle t_a \rangle$ and R . Agnello *et al.* [8] found these variables to be 1.25, 0.30, and 4×10^5 respectively. The use of such a method for determining the stopping cross section is likely to introduce additional uncertainties on top of the shaded region in Fig. 2, which is the uncertainty in the experimental measurements. According to Andersen and Ziegler [25] the fitting function described above has an estimated accuracy of 10% at 10 keV and 5% at 500 keV. However in the intermediate energy range the accuracy of the interpolation method is said to be approximately 20%. The restrictions of using a fitting function may be one possible explanation for the disagreement between our calculations and the experimental data.

V. CONCLUSION

In conclusion we have applied the CCC method to the calculation of stopping cross sections for antiprotons in the H_2 and H_2O molecules. For H_2 we fully account for the electron-electron correlation and average over all possible orientations of the target using an analytic orientation averaging technique. Double ionization and dissociative ionization contributions are also included via an independent-event model. Energy losses through vibrational excitation as well as the nuclear stopping cross section have been included. The presented theoretical results are the most comprehensive and the most accurate to date. We also presented the stopping cross section for antiprotons in H_2O . For the latter we used a neon-like model of six p -shell electrons above a frozen Hartree-Fock core with only one-electron excitations from the outer p shell allowed.

As a next step we plan to apply the CCC method to calculations of stopping cross sections for protons in atomic hydrogen. Due to the possibility of rearrangement, whereby the proton can grab an electron and form H, the aforementioned problem is significantly more difficult than its antiproton counterpart because it requires

a two-center expansion of the scattering wave function. Not only is the proton problem more complicated due to the need for a two-center expansion, one must also take into account all possible charged states of the projectile. This will ultimately require additional calculations of H/H^- scattering from H . With our current research in this direction our ultimate goal is to provide accurate calculations for radiation dose simulations in hadron therapy.

ACKNOWLEDGMENTS

This work was supported by the Australian Research Council, The Pawsey Supercomputer Centre, and the National Computing Infrastructure. A.S.K. acknowledges a partial support from the U.S. National Science Foundation under Award No. PHY-1415656.

-
- [1] D. Belkic, *Theory of Heavy Ion Collision Physics in Hadron Therapy*, Advances in quantum chemistry (Elsevier Science, 2012).
 - [2] J. W. Wilson, J. Miller, A. Konradi, and F. A. Cucinotta, eds., *Shielding Strategies for Human Space Exploration*, NASA conference publication 3360 (Langley Research Center; Hampton, VA, 1997).
 - [3] C. Bertulani, *Phys. Lett. B* **585**, 35 (2004).
 - [4] T. Kirchner and H. Knudsen, *J. Phys. B* **44**, 122001 (2011).
 - [5] M. H. Holzscheiter, N. Bassler, N. Agazaryan, G. Beyer, E. Blackmore, J. J. DeMarco, M. Doser, R. E. Durand, O. Hartley, K. S. Iwamoto, H. V. Knudsen, R. Landua, C. Maggiore, W. H. McBride, S. P. Mller, J. Petersen, L. D. Skarsgard, J. B. Smathers, T. D. Solberg, U. I. Uggerhj, S. Vranjes, H. R. Withers, M. Wong, and B. G. Wouters, *Radiotherapy Oncol.* **81**, 233 (2006).
 - [6] N. Bassler, J. Alsner, G. Beyer, J. J. DeMarco, M. Doser, D. Hajdukovic, O. Hartley, K. S. Iwamoto, O. Jkel, H. V. Knudsen, S. Kovacevic, S. P. Mller, J. Overgaard, J. B. Petersen, T. D. Solberg, B. S. Srensen, S. Vranjes, B. G. Wouters, and M. H. Holzscheiter, *Radiotherapy Oncol.* **86**, 14 (2008).
 - [7] A. Adamo, M. Agnello, F. Balestra, G. Belli, G. Bendiscioli, A. Bertin, P. Boccaccio, G. Bonazzola, T. Bressani, M. Bruschi, M. Bussa, L. Busso, D. Calvo, M. Capponi, C. Cicalò, M. Corradini, S. Costa, I. D'Antone, S. De Castro, F. D'Isep, A. Donzella, I. Falomkin, L. Fava, A. Feliciello, L. Ferrero, V. Filippini, D. Galli, R. Garfagnini, U. Gastaldi, P. Gianotti, A. Grasso, C. Guaraldo, F. Iazzi, A. Lanaro, E. Lodi Rizzini, M. Lombardi, V. Lucherini, A. Maggiora, S. Marcello, U. Marconi, G. Maron, A. Masoni, I. Massa, B. Minetti, M. Morando, P. Montagna, F. Nichitiu, D. Panzieri, G. Pauli, M. Piccinini, G. Piragino, M. Poli, G. Pontecorvo, G. Puddu, R. Ricci, E. Rossetto, A. Rotondi, A. Rozhdestvensky, P. Salvini, L. Santi, M. Sapozhnikov, N. Semprini Cesari, S. Serici, P. Temnikov, S. Tessaro, F. Tosello, V. Tretyak, G. Usai, L. Vannucci, G. Vedovato, L. Venturelli, M. Villa, A. Vitale, G. Zavattini, A. Zenoni, A. Zoccoli, and G. Zosi, *Phys. Rev. A* **47**, 4517 (1993).
 - [8] M. Agnello, G. Belli, G. Bendiscioli, A. Bertin, E. Botta, T. Bressani, M. Bruschi, M. Bussa, L. Busso, D. Calvo, B. Cereda, P. Cerello, C. Cicalò, M. Corradini, S. Costa, S. De Castro, A. Donzella, A. Feliciello, L. Ferrero, A. Filippi, V. Filippini, A. Fontana, D. Galli, R. Garfagnini, B. Giacobbe, P. Gianotti, A. Grasso, C. Guaraldo, F. Iazzi, A. Lanaro, E. Rizzini, V. Lucherini, S. Marcello, U. Marconi, A. Masoni, B. Minetti, P. Montagna, M. Morando, F. Nichitiu, D. Panzieri, G. Pauli, M. Piccinini, G. Puddu, E. Rossetto, A. Rotondi, A. Rozhdestvensky, A. Saino, P. Salvini, L. Santi, M. Sapozhnikov, N. Cesari, S. Serici, R. Spighi, P. Temnikov, S. Tessaro, F. Tosello, V. Tretyak, G. Usai, S. Vecchi, L. Venturelli, M. Villa, A. Vitale, A. Zenoni, and A. Zoccoli, *Phys. Rev. Lett.* **74**, 371 (1995).
 - [9] E. Lodi Rizzini, A. Bianconi, M. P. Bussa, M. Corradini, A. Donzella, L. Venturelli, M. Bargiotti, A. Bertin, M. Bruschi, M. Capponi, S. De Castro, L. Fabbri, P. Faccioli, D. Galli, B. Giacobbe, U. Marconi, I. Massa, M. Piccinini, M. Poli, N. Semprini Cesari, R. Spighi, V. Vagnoni, S. Vecchi, M. Villa, A. Vitale, A. Zoccoli, O. E. Gorchakov, G. B. Pontecorvo, A. M. Rozhdestvensky, V. I. Tretyak, C. Guaraldo, C. Petrascu, F. Balestra, L. Busso, O. Y. Denisov, L. Ferrero, R. Garfagnini, A. Grasso, A. Maggiora, G. Piragino, F. Tosello, G. Zosi, G. Margagliotti, L. Santi, and S. Tessaro, *Phys. Rev. Lett.* **89**, 183201 (2002).
 - [10] W. H. Barkas, J. N. Dyer, and H. H. Heckman, *Phys. Rev. Lett.* **11**, 26 (1963).
 - [11] H. Bethe, *Ann. Phys.* **397**, 325 (1930).
 - [12] W. H. Bragg and R. Kleeman, *Philos. Mag.* **10**, 318 (1905).
 - [13] A. Lühr and A. Saenz, *Phys. Rev. A* **79**, 042901 (2009).
 - [14] G. Schiwietz, U. Wille, R. D. Muio, P. Fainstein, and P. Grande, *Nucl. Instrum. Methods Phys. Res. B* **115**, 106 (1996).
 - [15] G. Schiwietz, U. Wille, R. D. Muio, P. D. Fainstein, and P. L. Grande, *J. Phys. B* **29**, 307 (1996).
 - [16] R. Cabrera-Trujillo, J. R. Sabin, Y. Öhrn, and E. Deumens, *Phys. Rev. A* **71**, 012901 (2005).
 - [17] J. J. Bailey, A. S. Kadyrov, I. B. Abdurakhmanov, D. V. Fursa, and I. Bray, *Phys. Rev. A* **92**, 022707 (2015).
 - [18] C. C. Montanari and J. E. Miraglia, *J. Phys. B* **47**, 015201 (2014).
 - [19] I. B. Abdurakhmanov, A. S. Kadyrov, D. V. Fursa, and I. Bray, *Phys. Rev. Lett.* **111**, 173201 (2013).
 - [20] I. B. Abdurakhmanov, A. S. Kadyrov, D. V. Fursa, S. K. Avazbaev, and I. Bray, *Phys. Rev. A* **89**, 042706 (2014).
 - [21] I. B. Abdurakhmanov, A. S. Kadyrov, D. V. Fursa, S. K. Avazbaev, J. J. Bailey, and I. Bray, *Phys. Rev. A* **91**, 022712 (2015).
 - [22] M. O. Abdellahi El Ghazaly, J. Jureta, X. Urbain, and P. Defrance, *J. Phys. B* **37**, 2467 (2004).
 - [23] T. E. Sharp, *At. Data Nucl. Data Tables* **2**, 119 (1970).
 - [24] G. A. Khayrallah, *Phys. Rev. A* **13**, 1989 (1976).
 - [25] H. Andersen and J. Ziegler, *Hydrogen stopping powers*

and ranges in all elements, Stopping and ranges of ions in matter (Pergamon Press, 1977).

[26] C. Varelas and J. Biersack, *Nucl. Instrum. Methods* **79**, 213 (1970).